Polym. Bull. (2018) 75:2105–2124
https://doi.org/10.1007/s00289-017-2127-7

ORIGINAL PAPER

Epoxy-silicone copolymer synthesis via efficient hydrosilylation reaction catalyzed by high-activity platinum and its effect on structure and performance of silicone rubber coatings

Bin Zhang[1] · Rui Li[1] · Jiemin Luo[1] · Yang Chen[1] · Huawei Zou[1] · Mei Liang[1]

Received: 28 March 2017 / Revised: 2 June 2017 / Accepted: 11 July 2017 /
Published online: 7 August 2017

Abstract In this study, two different pre-polymers were obtained first through efficient hydrosilylation reaction by changing reaction time and catalyst dosage in the presence of polyoxyethylene epoxy resin (DEG-501) and hydrogen silicone oil with phenyl (UC-233), named EH-F and EH-L. And the chemical structure of pre-polymers was confirmed by Fourier transform infrared spectroscopy and nuclear magnetic resonance (^{1}H-NMR). Then the pre-polymers were incorporated into phenyl-containing silicone rubber at different mass fractions. Scanning electron microscopy observations demonstrated that a "sea-island" phase separation occurred obviously in the cured composites. Thermogravimetric analysis evaluation revealed that thermal stability of silicone rubber composites improved markedly after modification, the residual yield at 800 °C achieved 32.69% in the air atmosphere when 20 phr EH-F were introduced. And a degradation mechanism was discussed through elemental analysis and electronic images of char of silicone rubber systems. The mechanical properties results showed that tensile strength and shear strength of composites increased gradually with increasing EH pre-polymers. All of these results provide very valuable information for understanding hydrosilylation reaction and effects of molecular structures on performance of silicone rubber systems.

✉ Huawei Zou
hwzou@163.com

Bin Zhang
1372194784@qq.com

Mei Liang
liangmeiww@163.com

[1] The State Key Lab of Polymer Materials Engineering, Polymer Research Institute of Sichuan University, Chengdu 610065, China

Keywords Silicone rubber · Polyoxyethylene epoxy ether · Hydrosilylation · Mechanical properties · Thermal properties · Adhesive properties

Introduction

Silicone polymers have attracted a great deal of interest of increasing number of researchers because of their excellent performance properties, such as superior thermal and thermo-oxidative stability, low temperature flexibility, good dielectric strength, water repellency, compressivity, doping action, and free rotation of chains about Si–O bonds and ease of manufacturing and shaping [1–5]. All these are required for their widespread and potential application as electrical and electronic equipment, medical treatment, air purification, corrosion-proof coatings and so on [4, 5].

However, it is acknowledged that the low surface free energy (19.9 mJ/m) and generally non-reactive, stable characteristics of silicone rubber limit their applications in industry and life as a commonly used adhesive agent [2]. Aiming at these problems, scientists have devoted to achieving surface modification and made huge progress, they usually increased surface energy and reactivity via the introduction of reactive functional groups onto the polymer surface through plasma treatment [6–20]. For example, Chantal Khan-Malek et al. [12] used conventional (oxygen plasma) and unconventional plasma modification (2-step modification using oxygen and C_2F_6) processes and also chemical grafting using oxygen plasma polymerization of 2-hydroxyethyl methacrylate (HEMA), the modification of surfaces were characterized using static contact angle measurements and attenuated total reflection Fourier transform infrared spectroscopy (ATR-FTIR) and it turned out to obtain stable hydrophilic surfaces. Nevertheless, a major drawback of plasma treatment is that the polydimethylsiloxane (PDMS) surface can be transformed into a brittle silica-like layer [11, 12, 21]. In addition, plasma treatment can only improve bonding performance but can not improve poor mechanical properties of silicone rubber.

While epoxy resin has many advantages including good adhesion performance and mechanical properties because of its special molecular chain structure. Introducing epoxy resin into liquid silicone rubber not only improves adhesion strength but also mechanical properties of silicone rubber. Therefore, some researchers studied properties of polydimethylsiloxane modified with epoxy resin. For example, Zhou et al. [3] synthesized a graft copolymer via condensation reaction between epoxy resin and polyorganosiloxane, then the synthetic copolymer was added into silicone rubber. The comprehensive performance of modified silicone rubber was studied and test results showed that the adhesion performance and mechanical properties, including thermal stability of silicone rubber composites increased. However, epoxy resin contains less hydroxyl functional groups and polyorganosiloxane has only a small amount of reactive functional groups, so the degree and efficiency of graft reaction is not high and complete. That is the molecular chain of epoxy resin grafted on the molecular chain of polyorganosiloxane is less. And some free epoxy still keep presence in the prepared material. Until now, according to our understanding, no papers have reported hydrosilylation reaction between polyorganosiloxane and epoxy resin. The reaction is about

carbon–carbon double bond of polyoxyethylene epoxy reacting with Si–H bond of hydrogen silicone oil with phenyl in the presence of noble metal catalyst. The two best advantages of this reaction are effectiveness and no byproducts. Consequently, we deem that the integrity of the reaction will introduce more epoxy groups and more rigid groups (hydrogen silicone oil with phenyl) to silicone rubber matrix, further enhancing bonding performance, mechanical properties and thermal stability. Before this, many researchers had committed to studying hydrosilylation reaction [22–26]. For instance, Min et al. [22] researched efficient routes to carbon–silicon bond formation for the synthesis of silicon-containing peptides and azasilaheterocycles, and concluded that Rh(I)-catalyzed double hydrosilylation protocol provides rapid access to molecules containing two carbon–silicon bonds.

In this work, we synthesized a precursor containing a segment of siloxane and a segment of polyoxyethylene epoxy, and it is a "*T*" type structure because of polyfunctionlization of hydrogen silicone oil with phenyl. Then, this copolymer was dispersed into the silicone rubber matrix with different mass fractions, and composites were crosslinked at room temperature for 7 days. The thermal, mechanical, adhesive properties and morphology of the silicone rubber modified by the copolymer have been investigated and the role of copolymer to properties improvement of silicone rubber systems has been also discussed in depth.

Experimental

Materials

Polyoxyethylene epoxy resin (DEG-501) was supplied by Zhangjiagang Tianrui Chemical Industry Co. Ltd, China. The hydrogen silicone oil with phenyl (UC-233, the viscosity is about 3000cst), was purchased from Jiaxing United Chemical Co. Ltd. Phenyl-containing silicone rubber, a kind of room temperature vulcanized silicone rubber (RTVSR) was bought from Shanghai Aishibo Silicone Material Co. Ltd. Dibutyltindiaurate (DTBDL), which was used as catalyst during the vulcanization, was supplied by Chengdu Chemical Reagent Company, China. The curing agent, 3-triethoxysilylpropylamine (APTES) was purchased kindly from China BlueStar Chengrand Research Institute of Chemical Industry. All of the materials utilized in this study were used directly without further purification.

Synthesis of siliconized epoxy resin (EH-F and EH-L)

DEG-501 (21.6 g) was first fed into a three-necked round-bottom flask equipped with reflux condenser, mechanical stirrer, and thermometer. Next, Argon was inlet to the three-necked round-bottom flask for almost 2 h on the grounds that it could exhaust air of glass bottle. Then, the catalyst named hexachloroplatinic acid was introduced into flask, and the mixture was stirred for another about 2 h at 50 °C. The blends were heated to 100 °C and hydrogen silicone oil with phenyl (UC-233) was added into the reaction bottle dropwise slowly. Finally, the reaction

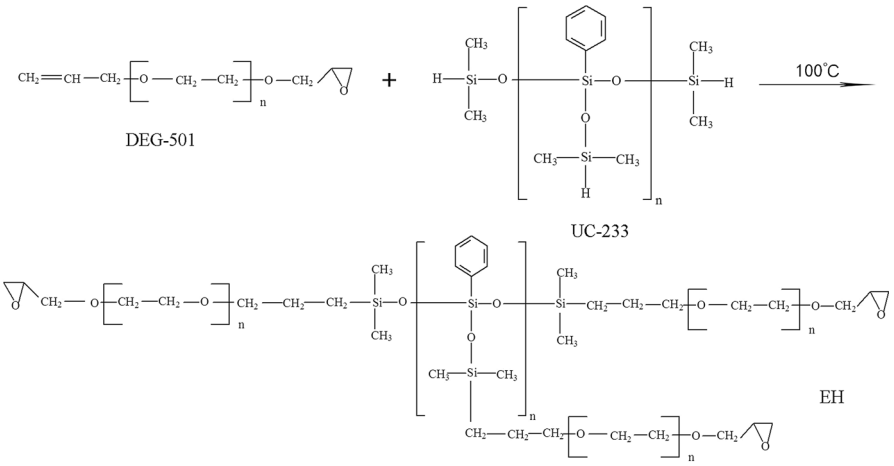

Scheme 1 Schematic representation of the preparation of siliconized epoxy resins (EH)

proceeded until it became a homogeneous viscous liquid under Argon atmosphere. The attained crude product was finally washed three times or more with toluene to remove the unreacted hydrogen silicone oil with phenyl (UC-233). The reaction procedure was certified in Scheme 1. The difference between EH-F product and EH-L product is amount of catalyst and reaction time in this synthesis process. The amount of catalyst and reaction time of synthesizing EH-F are 50 µl and 24 h, respectively. And that of synthesizing EH-L are 80 µl and 36 h, correspondingly.

Preparation process of silicone rubber composites with EH

Phenyl-containing silicone rubber matrix (12000cst) and EH (both EH-F and EH-L) were mixed in a beaker at 100 °C until it turned into well-distributed with the amounts of EH of 10, 20 and 30 phr. Next, the mixture was cooled to room temperature, a mixture of curing agent (APTES) and catalyst (DTBDL) were added into it. The liquid blends were entirely mingled by a mechanical stirrer and degassed with a vacuum pump to remove air bubbles. Then, the bubble-free mixtures were then poured into a polytetrafluoroethylene (PTFE) mold to manufacture samples. The curing reaction was carried out at room temperature for 7 days and the cured samples were prudently removed from the mold and reserved for different kinds of tests. Cured samples were assigned as Pure, EH-F-10, EH-F-20, EH-F-30, EH-L-10, EH-L-20 and EH-L-30 for more simple and intuitive description, denoting the amounts of pre-polymer in silicone rubber systems are 0, 10, 20 and 30 phr, respectively. The formulation of additive quantities of EH, APTES, and DTBDL employed in this work are listed in Table 1. The cure reaction of composites was certified in Scheme 2.

Table 1 Contents of the silicone rubber systems

Sample	EH (phr)	APTES (phr)	DTBDL (phr)
Pure	0	6	0.2
EH-F-10	10	6	0.2
EH-F-20	20	6	0.2
EH-F-30	30	6	0.2
EH-L-10	10	6	0.2
EH-L-20	20	6	0.2
EH-L-30	30	6	0.2

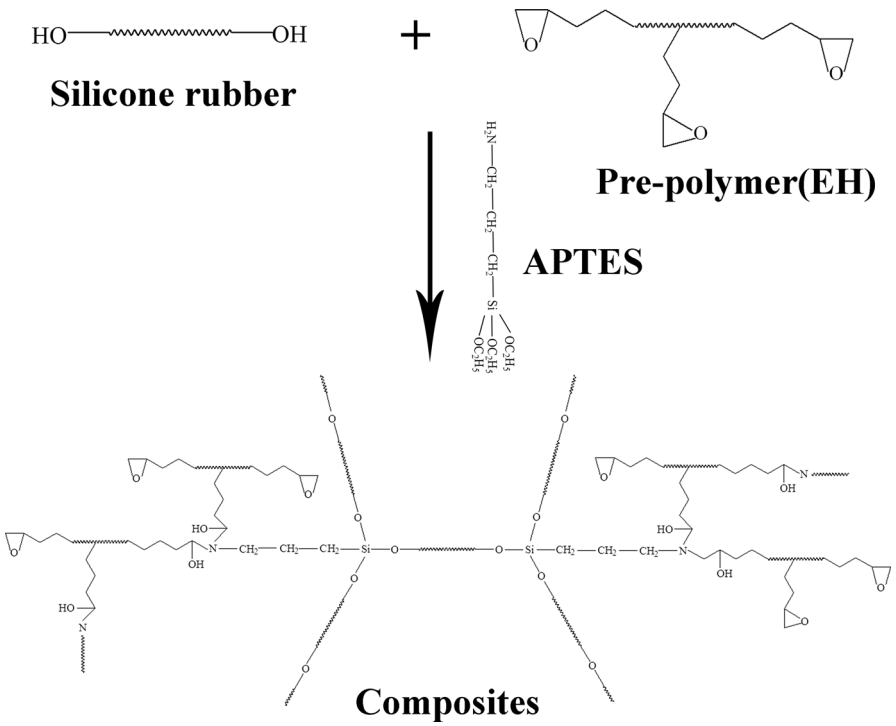

Scheme 2 Schematic representation of curing process of composites

Characterization

FTIR spectroscopy

A Nicolet 570 FTIR spectrophotometer (Nicolet, USA) with a resolution of 1 cm^{-1} was employed to cassetted Infrared spectra of DEG-501, UC-233 and EH in the range of 4000–400 cm^{-1}. The liquid samples were coated on different KBr disks polished very flat, respectively, and then the disks were set pad film and front and

rear frames. All prepared samples were put into card slot of instrument directly. All the samples were scanned from 4000 to 500 cm^{-1}.

^{1}H-NMR spectroscopy

The ^{1}H-NMR spectra of EH-F and EH-L were characterized. 3–8 mg sample (EH-F and EH-L) was added into two frozen tubes separately, and deuterated chloroform ($CDCl_3$) as solvent was injected in the two frozen tubes, then the two tubes were shaken for a few minutes, making sample dissolve into solvent and become colorless and transparent. Next, the two solutions were transferred into two nuclear tubes. And then the nuclear tubes were put in a 600 MHz DRX-600 NMR spectrometer (Bruker Company, Germany), the test was carried on at 25 °C.

Morphology of cured blends

The scanning electron microscope (SEM: JSM-5900, JEOL, Japan) was used to observe the morphology of the fracture surfaces at an accelerating voltage of 10 kV. Samples were soaked in liquid nitrogen for about 12 h, making them change from rubber state to glass state, next these samples below glass state were broken to two flat surfaces. Then samples were stuck to conductive film and fracture surfaces were upward vertically. To enhance conductivity and prevent charging, we coated with gold for the surfaces of all the specimens before the observation. All these samples were observed for different multiple.

Thermogravimetric analysis(TGA)

The thermogravimetric analyzer (TG 209F1 Iris, Netzsch, Germany) was needed to consider the thermal stability of the specimens. The specimens were weighed between 3 and 10 mg, and then were put into each clean crucible. All the crucibles were sent to fixed position by test instrument automatically. Then thermal stability of the specimens was tested under dry nitrogen and air atmosphere separately with a velocity of flow of 60 ml/min. The samples were heated at a rate of 10 °C/min. And the related mass loss of the specimens was recorded at the range of 50–800 °C.

Mechanical properties

According to ISO 37:2011, the tensile strength and elongation at break of the cured samples with the dumbbell-shaped were tested with an Instron (Instron 5567, Instron, USA) universal testing instrument at a rate of 500 mm/min. The cured films were cut into strips of 100 mm × 5 mm in size. Before testing, test specimens were examined for each composition and the two ends of samples were fixed on small pneumatic fixture with a sensor, and machine load (stress and strain loads) was return to zero. The tensile strength was considered as mean of five highest readings at peak load. Elongation at break was deemed strain values at the breaking point. All mechanical behavior was carried out with an average of five specimens.

Adhesion properties

According to ISO 4587:2003, the shearing strength of cured specimens was measured by Instron universal tensile instrument (Instron 5567). Tested samples were coated on two aluminum sheet substrate with wiping clean after grinding, then the two aluminum sheet were glued together by a lapping way, and samples vulcanized naturally at room temperature. The size of all tested samples was unified in 25 mm × 12.5 mm. The test was conducted at a speed of 5 mm/min at room temperature. All adhesion behaviors were carried out with an average of five specimens.

Results and discussion

Characterization of siliconized epoxy resins (EH-F and EH-L)

The FTIR and ^{1}H-NMR were used to characterize the structure of EH-F, EH-L, DEG-501 and UC-233, and the spectra were shown in Figs. 1 and 2. From Fig. 1, it can be seen that characteristic peak of Si–H of UC-233 at about 2134 cm^{-1} is very strong, but it disappears in the FTIR spectra of EH-L, and the peak intensity of it becomes weak extremely in the FTIR spectra of EH-F. The signal of C=C groups at almost 1637 cm^{-1} is still observed in the FTIR spectra of EH-F and EH-L, and its peak intensity is weaker exceedingly than DEG-501. The stretching vibration of Si–O–Si appears at the range from 1210 to 1050 cm^{-1} in the FTIR spectra of EH-F and EH-L. These results suggest hydrosilylation. In addition, some other absorption peaks in the infrared spectra are also identified containing 2959, 1428 cm^{-1} (Si–CH_3), 3068 cm^{-1} (=C–H), 2855 cm^{-1} (−CH_2–), 1600, 1460, 1490 cm^{-1} (Si–

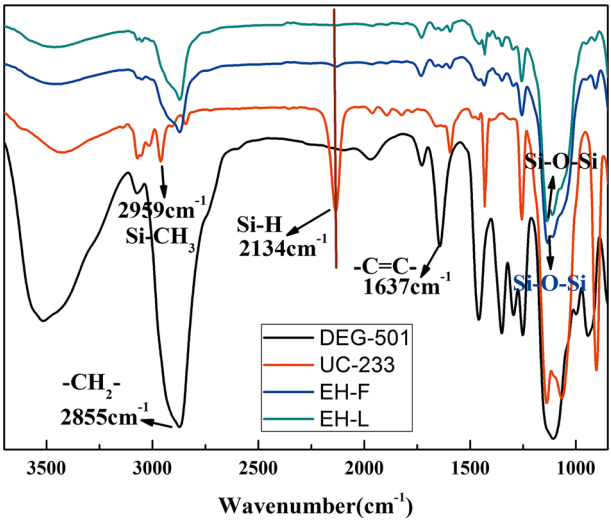

Fig. 1 FTIR spectra of DEG-501, UC-233, EH-F and EH-L

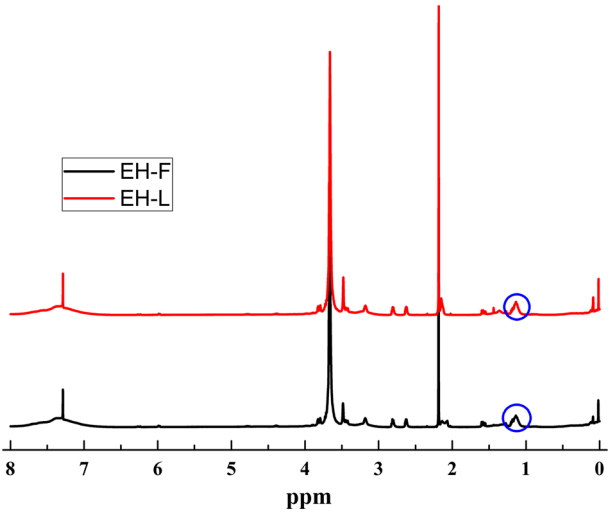

Fig. 2 ^{1}H-NMR spectra of EH-F and EH-L

phenyl), 910 cm^{-1} (oxirane). According to ^{1}H-NMR shown in Fig. 2, the signal at 1.1 ppm is attributed to Si-CH_2, indicating that success of the reaction between DEG-501and UC-233. The peaks at 2.3–3.6 ppm belong to –CH_2. The signal of 7.26 ppm is ascribed to aromatic ring protons. These results further demonstrate the formation of target product.

Morphology of fracture surface of the silicone rubber systems

The morphology of fracture surface of cured silicone rubber systems were characterized by scanning electron microscope (SEM), and the corresponding photos are shown in Fig. 3. From the picture, it is obvious that a phase separation called "sea-island" structure occurs in all composites and smooth and flat surface exists in the pure matrix. This can be attributed to introducing EH pre-polymers. However, for EH-F, it can be seen that the size of particles of EH-F-10 are small, and they distribute unevenly in the substrate. When more phr of EH-F were blended with silicone rubber, the morphology of fracture surface of composites (EH-F-20 and EH-F-30) become different from that of EH-F-10, the size of dispersed phase increase, and the average diameter of them is 5–7 μm. Surprisingly, the fracture surface of EH-F-30 displays similar dispersed phase structure compared to EH-F-20 from photograph, the size of dispersed phase EH-F-30 has no significant increase with increasing EH-F. This maybe, to some extent, enhancement of the compatibility between EH-F-30 and silicone rubber substrate.

For EH-L, it can be noticed that the size of dispersed phase is smaller compared to EH-F, and EH-L-10 performs more clearly. In the process of synthesizing EH-F, the reaction between carbon–carbon double bond of polyoxyethylene epoxy and Si–H bond of hydrogen silicone oil with phenyl is not complete, and the Si–H is residual. But in the process of synthesizing EH-L, the reaction between carbon–

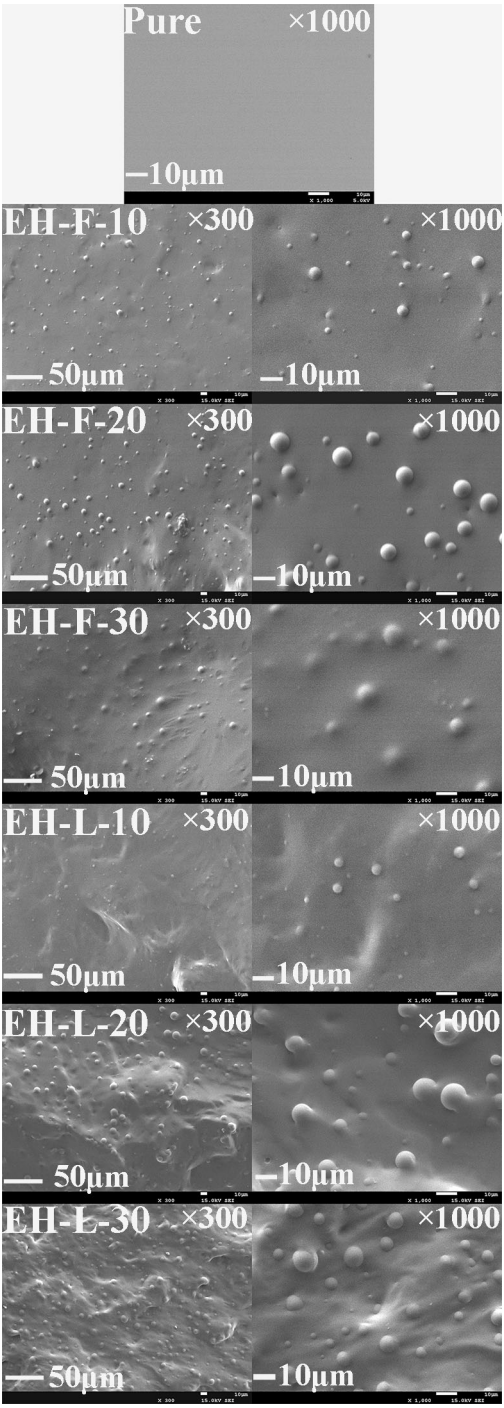

Fig. 3 The SEM of the silicone rubber systems with different contents of EH on the *left* at ×300: and on the *right* at ×1000: Pure, EH-F-10, EH-F-20, EH-F-30, EH-L-10, EH-L-20, EH-L-30

carbon double bond of polyoxyethylene epoxy and Si–H bond of hydrogen silicone oil with phenyl is complete, and there is no Si–H left. This can be also proved by FTIR spectra result. Like EH-F composites, EH-L composites present similar variation trend, the size of dispersed phase existing in the silicone rubber systems are small, and become large when 20 and 30 phr pre-polymers are added into base rubber. The siloxane part of siliconized epoxy resin (EH) acts as an effective compatibilizer and the reaction between vulcanizing agent (APTES) (alkoxy group and amino group) and silicone rubber systems (hydroxyl and epoxy group) make great contribution to good compatibility between EH and phenyl-containing silicone rubber [3].

TGA analysis of the cured silicone rubber systems

The thermal stability of the cured silicone rubber composites was investigated by thermogravimetric analysis (TGA) under both nitrogen and air atmospheres. And the specific data of TGA and DTG curves are listed detailedly in Tables 2 and 3. As is shown in Fig. 4a, in nitrogen atmosphere, the pure silicone rubber has a very small amount of volatiles when the temperature under 217 °C, as the temperature increases, mass loss increases obviously and a large quantity of volatiles produced until 1.71% residue is left at 800 °C. However, when some EH pre-polymers were introduced into composite systems, heat-resistance of composites is better than the neat matrix. The initial thermal degradation temperature ($T_{5\%}$) of complex systems increase, especially EH-F-30 composites perform the highest onset degradation temperature, almost reaching 264 °C. This can be ascribed to higher steric hindrance of phenyl groups of UC-233, hampering movement of molecular chains, further blocking Si–O bonds' rearrangement via kinetically favored paths [27–31]. However, the onset thermal degradation temperature of EH-F-20 and EH-L-20 has a drop, this is because the onset temperature of composites is decided by two reasons. First, high steric hindrance of phenyl groups of UC-233 added into the matrix in the form pre-polymer [27–31], causing the onset temperature to increase. Second, the rigidity of composites influences crosslinking reaction of themselves [30], causing the onset temperature to decrease. Therefore, There is a competition between the two factors, for EH-F-10 (or EH-L-10), high steric hindrance of phenyl groups has brought a obvious effect, but for EH-F-30 (or EH-L-30) (higher steric hindrance of phenyl groups), the influence of incomplete crosslinking reaction due to strong

Table 2 TGA data of the silicone rubber systems under nitrogen atmosphere

Sample	T_{onset} (°C)	T_{max} (°C)	R_{800} (%)
Pure	217.0	364.9/540.6	1.71
EH-F-10	246.4	413.0/569.9	9.92
EH-F-20	238.9	430.4/561.1	11.26
EH-F-30	264.4	428.4/562.2	8.35
EH-L-10	254.4	433.2/564.4	6.23
EH-L-20	233.9	442.4/564.6	10.99
EH-L-30	258.8	434.2/564.2	10.22

Table 3 TGA data of the silicone rubber systems under air atmosphere

Sample	T_{onset} (°C)	T_{max} (°C)	R_{800} (%)
Pure	228.8	459.3/559.4	16.96
EH-F-10	238.9	456.8/665.6	25.97
EH-F-20	264.1	459.4/677.7	32.69
EH-F-30	256.1	446.7/662.1	21.43
EH-L-10	281.0	461.2/679.6	28.69
EH-L-20	251.0	453.8/672.1	25.36
EH-L-30	208.5	483.9/682.5	20.67

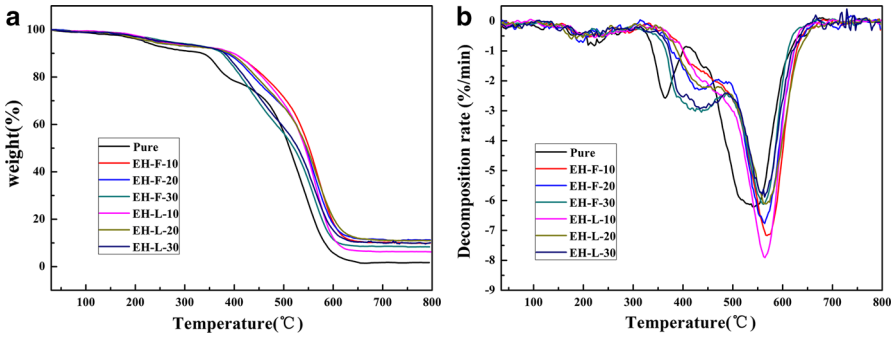

Fig. 4 TGA (**a**) and DTG (**b**) curves of silicone rubber composites in nitrogen atmosphere

rigidity is more obvious than that of high steric hindrance of phenyl groups. So the onset temperature of EH-F-10 (or EH-L-10) is higher than EH-F-30 (or EH-L-30). However, for EH-F-20 (or EH-L-20), the steric hindrance of phenyl groups is lower than EH-F-30 (or EH-L-30), and the influence of incomplete crosslinking reaction due to strong rigidity is higher than EH-F-10 (or EH-L-10), so the onset temperature of EH-F-20 (or EH-L-20) is lower than that of EH-F-10 (or EH-L-10) and EH-F-30 (or EH-L-30). From Fig. 4b, it can be seen that degradation processes of composites conclude two key steps. First, "Unzipping degradation" of molecular chain end of silicone rubber systems due to residual terminal hydroxyl groups lead to Si–O scission and a small part weight loss, producing siloxane cyclopolymers. Second, at higher temperature, formed siloxane cyclopolymers in the first stage degrade continuously, generating small molecules and formed rings being destroyed. In addition, Si–CH_3 scission also happens at this stage, so making mass of materials lost quickly [3, 27–34]. When EH pre-polymers were into the pure silicone rubber, the temperature of maximum weight loss (T_{max}) increase and mass loss at the same temperature decrease of composites compared with the neat matrix. Degradation residues of at 800 °C of composite materials increase after pre-polymers were mixed with silicone matrix. This is mainly because more phenyl groups exist in complex materials, which can promote the formation of carbon residues and make the carbon residue layer become dense. Surprisingly, the residue of silicone rubber systems decrease when 30 phr of EH precursors (higher phenyl content compared

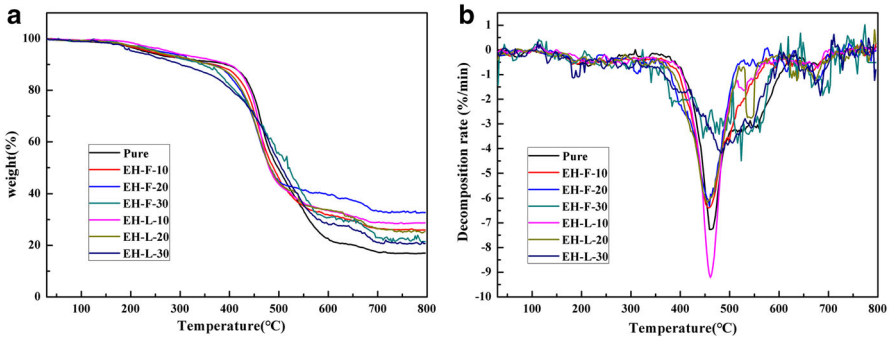

Fig. 5 TGA (**a**) and DTG (**b**) curves of silicone rubber composites in air atmosphere

with 10 phr of EH precursors or 20 phr of EH precursors) were added into silicone rubber substrate. This may be at higher temperature, due to the effect of Si–OH bond, Si–Ph bond scission is faster than Si–CH_3 bond cleavage. With the fracture of the Si–Ph bond, the rate of Si–O bond scission of the silicone rubber with high phenyl content is faster than that of the ones with low phenyl content [31]. Therefore, the residues decrease with increasing content of EH. From Fig. 5, it can be clearly seen that the onset decomposition temperature of composites increase with joining the pre-polymers, strangely, whether it is in EH-F composites or EH-L composites, the initial decomposition temperature of them decreases with more pre-polymers being added. This can be attributed to the rigidity of EH-F-30 and EH-L-30 composites are so strong that the crosslinking reaction (producing water through terminal hydroxyl groups) in the curing process is incomplete, meaning that cured EH-F-30 and EH-L-30 composites have more residual hydroxyl groups than other

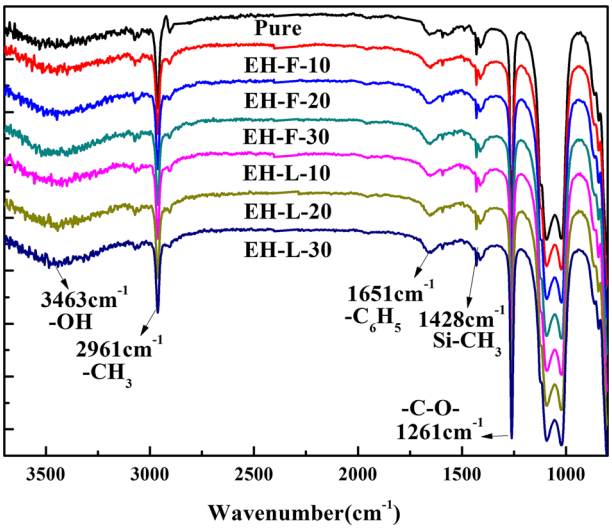

Fig. 6 FTIR spectra of cured composites

cured silicone rubber [30]. And this can be demonstrated by Fig. 6. With the increasing of temperature, the mobility of backbone will increase, the mobility of residual Si–OH groups will increase and react again with each other. In the degradation process, residual hydroxyl groups of EH-F-30 and EH-L-30 composites have more chances to undergo a dehydration reaction at high temperature [30]. On the other hand, residual hydroxyl groups have been proved to promote the cleavage of Si–O and Si–Ph bond [31], so degradation of EH-F-30 and EH-L-30 composites caused by these reactions is more remarkable than other silicone rubber hybrids. In addition, it can be seen clearly the onset temperature of EH-L-30 is low compared to pure composite, this can be explained in air atmosphere, it has been reported that the interaction of oxygen with polysiloxane depends on the diffusion and solubility of oxygen in polysiloxane [27]. When EH-L-30 were added into matrix, more Si–ph exist in composites, these rigid groups can occur interreaction in air, leading to cleavage of the Si–phenyl bond of pre-polymer including the matrix itself [31]. And these new generated small molecules are extremely unstable and easily react with oxygen, producing volatile small molecules [28]. The temperature of maximum weight loss (T_{max}) of EH complex materials in air atmosphere are higher than that in nitrogen atmosphere. This can be explained that scission of the Si–phenyl bond and subsequent proton abstraction to form benzene or dehydrogenation among phenyl to form condensed aromatic structure takes place at higher temperatures in air atmosphere [31]. Degradation residues of at 800 °C of composite materials in air are higher compared with residues at 800 °C of EH materials in N_2. This is because it was reported that the thermal oxidative degradation of polysiloxane depends on the diffusion and solubility of oxygen in polysiloxane [27]. The introduction of phenyl groups lead to the formation of a network that is ordered which can firmly bound molecular chains of composites, and the regions inhibit the diffusion and solution of oxygen in polymers [30]. Therefore, more residues are reserved.

Elemental analysis and electronic images of char of silicone rubber composites

To investigate the change of element content of char of cured samples, EDS was employed to perform for this purpose, and the result is shown in Table 4 and Fig. 7. From this result, the carbon content is about 8.60, 7.07, 8.03% and silicon content is about 23.38, 25.64, 25.12% in the neat matrix, EH-F-20 composites and EH-L-10

Table 4 Element concentration of the exterior char of silicone rubber composites by EDS (%)

Sample	C	O	Si
Pure	8.60	68.02	23.38
EH-F-10	8.42	65.60	25.98
EH-F-20	7.07	67.29	25.64
EH-F-30	7.65	66.62	25.73
EH-L-10	8.03	66.86	25.12
EH-L-20	8.20	67.02	24.79
EH-L-30	13.63	65.99	20.38

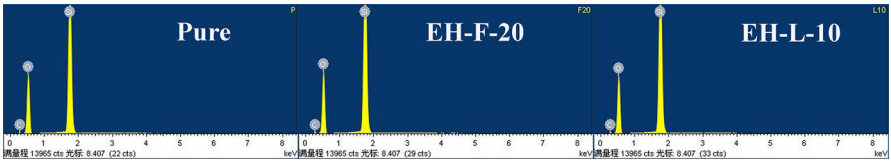

Fig. 7 Element analysis pictures of pure sample, EH-F-20 and EH-L-10 composites

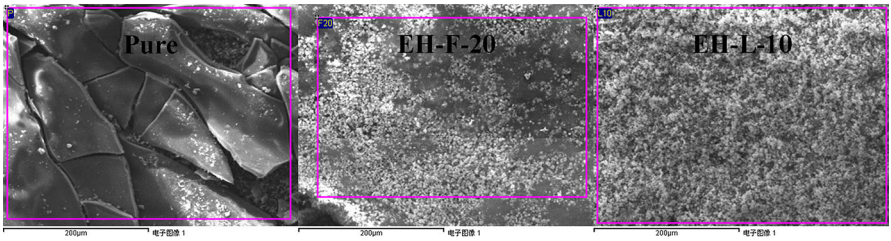

Fig. 8 Electronic images of char of pure matrix, EH-F-20 and EH-L-10 silicone rubber composites

composites, respectively. From Table 4, it can be seen that the carbon content in EH-F composites decreases but the silicon content increases compared to neat. Among EH-F complex materials, when amounts of pre-polymer increase, the carbon content decreases first and then increases, and this tendency is consistent with change of silicon content. For EH-L composites, the carbon content increases always, and the silicon content decreases conversely with increasing EH-L. These results reveal degradation process of EH-F and EH-L composites is a little different. This agrees with TGA analysis that variety discipline of carbon residues of EH-F silicone rubber systems is not same with that of EH-L silicone rubber systems. From Fig. 5, after the thermal oxygen degradation stages finish, EH-F-20 hybrids have the highest char for EH-F composites and EH-L-10 hybrids have the highest char for EH-L composites, revealing silicone-containing structures are mostly preserved in the char layers. From Fig. 8, it can be clearly observed that char layer of the pure silicone rubber is not continuous and compact, and there are many fragments and some white powders (silica), so it cannot prevent heat flow and protect internal materials. However, the char layer of EH-F-20 and EH-L-10 composites is dense, intact and successive, and the surface of char layer is white silica. Therefore, it can be speculated that the char layer is hard because of producing silicon carbide substances during high oxidation as a result of introducing EH pre-polymers. This again confirms that the improvement of thermal stability of modified silicone rubber.

Analysis of thermal degradation mechanism of silicone rubber systems

The thermal decomposition diagrams of pure sample and modified silicone rubber composites are simulated and the result is shown in Fig. 9. From this schematic diagram, it can be seen that unzipping and random thermal degradation reactions are key decomposition stages of the pure silicone rubber, producing cyclic small

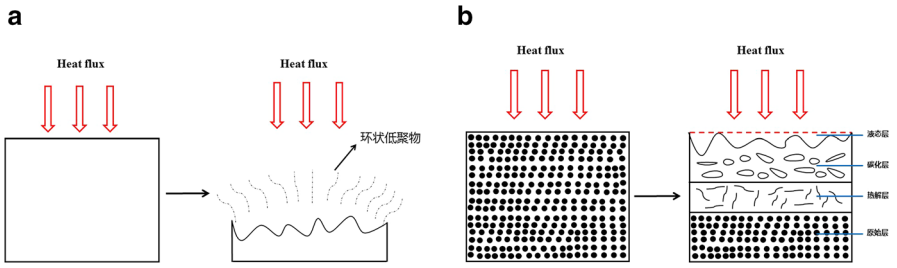

Fig. 9 Thermal damage mechanism diagrams of pure (**a**) and silicone rubber systems (**b**)

Scheme 3 The main reaction equations existing in the carbonized layer during thermal degradation of silicone rubber composites

$$SiO_2\ (l) + 3C \longrightarrow SiC\ (s) + 2\ CO$$

$$SiO_2\ (l) + 2C \longrightarrow Si\ (l) + 2\ CO$$

$$SiO_2\ (l) + C \longrightarrow SiO\ (g) + CO$$

molecules. Then these generated substances escape and the remaining SiO_2 are sparse. However, after EH pre-polymers are introduced into matrix, siliconized epoxy resin can provide carbon sources that can react with siloxane, generating high temperature-resistance substances when silicone rubber composites are subject to heat treatment. As is shown in Fig. 9b, silicone rubber systems present different degradation stage layers from the outside to the inner. The first layer is liquid layer, it can contact high temperature hot air flow or open fire, and produce liquefied organic matter and liquid silica. The second layer is carbonized layer, in this layer, pyrolytic carbon from the heat treatment of EH can react with SiO_2 from decomposition of matrix, generating dense shield effect. Some main reaction equations are shown in Scheme 3. The third layer is pyrolysis layer, the internal material itself begins to decompose when heat transfer happen from outside to inside, and produce small molecules, leading to some small holes in the layer. The bottom layer is original layer that can be protected by above layers, so it is affected by thermal degradation next to nothing. But it can decompose subsequently with increasing time of heat treatment. Thermal decomposition mechanism diagrams reveal reasons of the improvement of thermal stability of silicone rubber systems.

Mechanical properties

The influence of EH content on tensile strength and elongation at break are discussed, and test results are shown in Fig. 10. For EH-F composite systems, it can be clearly seen that the tensile strength increases first and then decreases with increasing content of EH-F. When 10 wt% EH-F is introduced, the tensile strength reaches 0.127 MPa, near 2-times of neat silicone rubber, this is because rigid groups (benzene ring) of UC-233 are brought into hybrids, making ability of withstanding external stress increase [3]. A decrease in the tensile strength of EH-F-20 and EH-F-

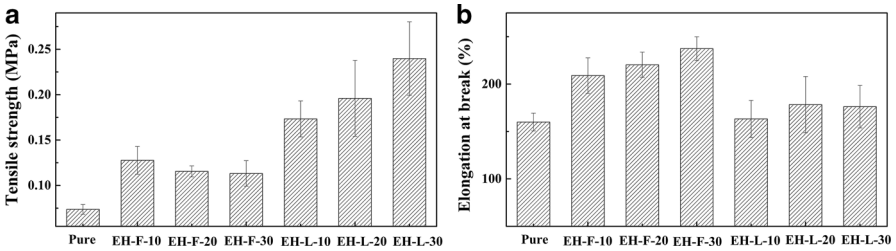

Fig. 10 Tensile strength (**a**) and elongation at break (**b**) of silicone rubber composites with different amounts of EH

30 composites is explained that the bigger particles act as stress concentration point, and the materials are destroyed easily along the crack when they subject to experimental pulling force. For EH-L composite systems, the tensile strength of them is much higher than EH-F composite systems, and variation tendency that the tensile strength is a function of the added amounts of pre-polymers is different from EH-F composite systems. When 10 phr of EH-L are mixed with silicone rubber, the value of tensile strength is 0.174 MPa, higher than EH-F-30 sample. Moreover, tensile strength increase continuously with increasing the EH-L content, and the peak value is 0.24 MPa. This can be ascribed to the size of dispersed phase is little, with mass percentages of EH-L increasing gradually, more granular balls appear in the composite systems, and they can play a stress transmitter when these samples are tested by universal testing machine, so leading to not be damaged lightly. This is certified by FTIR spectra result, illustrating that degree of reaction of EH-L is better than EH-F.

As shown in Fig. 10b, it is very clear to see that the elongation at break of EH-F composites improve progressively with enhancing content of EH-F, and achieves 237% with 30 phr of EH-F pre-polymers being added while the value of pure sample is only 160%. As is known, polarity and conformation of molecular chains dominate flexibility of materials, determining the elongation at break. For EH-F silicone rubber systems, the molecular chains change from a curled state to an extended state when they are born pull, then prolong continuously and until break off. That is molecular chains can deform randomly so as to refused to be devastated. However, due to reaction level of EH-L is better than EH-F, meaning that more epoxy groups are embedded into composite materials and they are cured by amino groups of APTES, so crosslinking density of three-dimensional network of EH-L hybrids is larger than that of EH-F hybrids [35–37]. Therefore, the molecular chains of EH-L materials cannot stretch freely, it is easy to be damaged for materials when they subject to external stress [38, 39]. Consequently, there is no change for the elongation at break of EH-L silicone rubber materials compared to pure matrix.

Adhesion properties

For coatings, adhesion is a significant property. As is shown in Fig. 11, it can be seen that the shear strength of EH-F composite materials increase slowly, and only

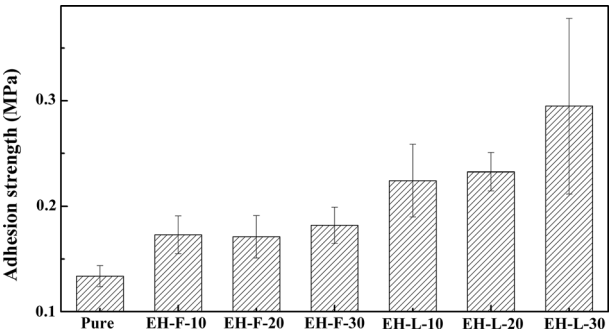

Fig. 11 The adhesion properties of silicone rubber composites

reach 0.174 MPa by adding 10 phr EH-F pre-polymers. In accordance with that of tensile strength, the change of adhesion strength is indistinct when more quantities of EH-F are preserved in this complex system. This is mainly because the mechanical strength determines the bonding strength. It is easy to be destructed when materials are suffered mechanical power, thus losing adhesion property to protected material surfaces. Therefore, for EH-L complex materials, the shear strength of them increases gradually with increasing content of EH-L. This change is consistent with change in tensile strength. Enhancement of shear strength of EH-L composites is attributed to three reasons. On one hand, epoxy resin chains can interact with matrix via hydrogen bond and epoxy group [40]. More additions of EH-L can bring more epoxy groups. On the other hand, the improvement of mechanical properties could generate much more viscous dissipation than unmodified silicone rubber systems [3]. And finally, epoxy groups of EH can react with amino group in APTES, improving interface performance [41]. In addition, APTES is a general silane coupling agent and adhesion promoter, so it can improve adhesion strength [42–44].

Conclusion

Novel silicone-epoxy pre-polymers named EH-F and EH-L were successfully prepared via hydrosilylation reaction and characterized by FTIR and ^{1}H NMR. The FTIR result indicates reaction degree of EH-F and EH-L is not identical, and reactivity of EH-L is better than that of EH-F. Scanning electron microscopy (SEM) techniques indicate a phase separation occurs between silicone rubber matrix and precursors, and the size of dispersed phase becomes large with more pre-polymers were added. The thermal stability of modified composites was significantly improved. And thermal stability of silicone rubber systems under air atmospheres is better than that in nitrogen atmospheres. Elemental analysis results show that silicon content increases and carbon content decreases for modified silicone rubbers compared with the pure matrix. And there are more carbon residue substances similar to ceramics that are hard and dense covering composites substrate.

Mechanical properties tests demonstrate that the tensile strength of EH-L hybrids is superior to that of EH-F hybrids and is much higher than that of the pure silicone rubber. But the elongation at break of EH-F silicone rubber composites is better than that of EH-L silicone rubber composites, these results are related to degree of reaction precursors. Adhesion properties measurements reveal that the shear strength of composites increase after the silicone rubber matrix was mixed with EH pre-polymers.

All these results proved that it was important to modify phenyl-containing silicone rubber with EH. It is believed that the composites may be probably used as heat-resistant coatings and high temperature bonding materials.

Acknowledgements The author(s) disclosed receipt of the following financial support for the research, authorship, and/or publication of this article. The authors would thank the National Natural Science Foundation of China (51273118) for financial support, and the Analytical and Testing Center of Sichuan University for providing SEM observation.

References

1. Dong FY, Diao S, Ma DP, Zhang SY, Feng SY (2015) Preparation and characterization of 3-chloropropyl polysiloxane-based heat-curable silicone rubber using polyamidoamine dendrimers as cross-linkers. React Funct Polym 96:14–20
2. Wang XL, Dou WQ (2012) Preparation of graphite oxide (GO) and the thermal stability of silicone rubber/GO nanocomposites. Thermochim Acta 529:25–28
3. Zhou C, Li R, Luo W, Chen Y, Zou HW, Liang M (2016) The preparation and properties study of polydimethylsiloxane-based coatings modified by epoxy resin. J Polym Res 23:14
4. Zhu C, Deng C, Cao JY, Wang YZ (2015) An efficient flame retardant for silicone rubber: preparation and application. Polym Degrad Stab 121:42–50
5. Chang CL, Don TM, Lee HS-J, Sha Y-O (2004) Studies on the aminolysis of RTV silicone rubber and modifications of degradation products. Polym Degrad Stab 85:769–777
6. Pinto S, Alves P, Matos CM, Santos AC, Rodrigues LR, Teixeira JA, Gil MH (2010) Poly (diethyl siloxane) surface modification by low pressure plasma to improve its characteristics towards biomedical applications. Colloid Surf B 81:20–26
7. Abbasi F, Mirzadeh H, Katbab A (2001) Modification of polysiloxane polymers for biomedical applications: a review. Polym Int 50:1279–1287
8. Sia SK, Whitesides GM (2003) Microfluidic devices fabricated in poly(dimethylsiloxane) for biological studies. Electrophoresis 24:3563–3576
9. Williams RL, Wilson DJ, Rhodes NP (2004) Stability of plasma-treated silicone rubber and its influence on the interfacial aspects of blood compatibility. Biomaterials 25:4659–4673
10. Cordeiro AL, Nitschke M, Janke A, Helbig R, D'Souza F, Donnelly GT, Willemsen PR, Werner C (2009) Fluorination of poly(dimethylsiloxane) surfaces by low pressure CF4 plasma -physicochemical and antifouling properties. Express Polym Lett 3:70–83
11. Sugiura S, Edahiro J, Sumaru K, Kanamori T (2008) Surface modification of polydimethylsiloxane with photo-grafted poly(ethyleneglycol) for micropatterned protein adsorption and cell adhesion. Colloid Surf B 63:301–305
12. Bodas D, Malek CK (2006) Formation of more stable hydrophilic surfaces of PDMS by plasma and chemical treatments. Microelectron Eng 83:1277–1279
13. Boxshall K, Wu MH, Cui Z, Cui ZF, Watts JF, Baker MA (2006) Simple surface treatments to modify protein adsorption and cell attachment properties within a poly(dimethylsiloxane) microbioreactor. Surf Interface Anal 38:198–201
14. Mikhail AS, Jones KS, Sheardown H (2008) Dendrimer-grafted cell adhesion peptide-modified PDMS. Biotechnol Prog 24:938–944

15. Karkhaneh A, Mirzadeh H, Ghaffariyeh AR (2007) Simultaneous graft copolymerization of 2-hydroxyethyl methacrylate and acrylic acid onto polydimethylsiloxane surfaces using a two-step plasma treatment. J Appl Polym Sci 105:2208–2217
16. McDonald JC, Duffy DC, Anderson JR, Chiu DT, Wu HK, Schueller OJA, Whitesides GM (2000) Fabrication of microfluidic systems in poly(dimethylsiloxane). Electrophoresis 21:27–40
17. Lippens E, Smet ND, Schauvliege S, Martens A, Gasthuys F, Schacht E, Cornelissen R (2012) Biocompatibility properties of surface-modified poly(dimethylsiloxane) for urinary applications. J Biomater Appl 27:651–660
18. Xiao D, Zhang H, Wirth M (2002) Chemical modification of the surface of poly(dimethylsiloxane) by atom-transfer radical polymerization of acrylamide. Langmuir 18:9971–9976
19. Ren XQ, Bachman M, Sims C, Li GP, Allbritton NJ (2001) Electroosmotic properties of microfluidic channels composed of poly(dimethylsiloxane). J Chromatogr B Biomed Sci Appl 762:117–125
20. Seitz V, Arzt K, Mahnel S, Rapp C, Schwaminger S, Hoffstetter M, Wintermantel E (2016) Improvement of adhesion strength of self-adhesive silicone rubber on thermoplastic substrates—comparison of an atmospheric pressure plasma jet (APPJ) and a Pyrosil® flame. Int J Adhes Adhes 66:65–72
21. Eddington DT, Puccinelli JP, Beebe DJ (2006) Extended curing and reduced hydrophobic recovery of polydimethylsiloxane. Sens Actuators B 114:170–172
22. Min GK, Hernandez D, Skrydstrup T (2013) Efficient routes to carbon–silicon bond formation for the synthesis of silicon-containing peptides and azasilaheterocycles. Acc Chem Res 46:457–470
23. Van DD, Hosokawa T, Saito M, Horiuchi Y, Matsuoka M (2015) A heterogeneous mesoporous silica-supported cyclopentadienyl ruthenium(II) complex catalyst for selective hydrosilylation of 1-hexyne at room temperature. Appl Catal A 503:203–208
24. Revunova K, Nikonov GI (2014) Base-catalyzed hydrosilylation of ketones and esters and insight into the mechanism. Chem A Eur J 20:839–845
25. Xu YS, Bai Y, Peng JJ, Li JY, Xiao WJ, Lai GQ (2014) Hydrosilylation of alkenes catalyzed by rhodium with polyethylene glycol-based ionic liquids as ligands. J Organomet Chem 765:59–63
26. Sumida Y, Kato T, Yoshida S, Hosoya T (2012) Palladium-catalyzed regio- and stereoselective hydrosilylation of electron-deficient alkynes. Org Lett 14:1552–1555
27. Caminoa G, Lomakin SM, Lazzari M (2001) Polydimethylsiloxane thermal degradation. Part 1. Kinetic aspects. Polymer 42:2395–2402
28. Camino G, Lomakin SM, Lageard M (2002) Thermal polydimethylsiloxane degradation. Part 2. The degradation mechanisms. Polymer 43:2011–2015
29. Deshpande G, Rezac ME (2001) The effect of phenyl content on the degradation of poly(dimethyl diphenyl) siloxane copolymers. Polym Degrad Stab 74:363–370
30. Yang ZZ, Han S, Zhang R, Feng SY, Zhang CQ, Zhang SY (2011) Effects of silphenylene units on the thermal stability of silicone resins. Polym Degrad Stab 96:2145–2151
31. Zhou WJ, Yang H, Guo XZ, Lu JJ (2006) Thermal degradation behaviors of some branched and linear polysiloxanes. Polym Degrad Stab 91:1471–1475
32. Liu YR, Huang YD, Liu L (2007) Influences of monosilanolisobutyl-POSS on thermal stability of polymethylsiloxane. J Mater Sci 42:5544–5550
33. Mutin PH (1999) Control of the composition and structure of silicon oxycarbide and oxynitride glasses derived from polysiloxane precursors. J Sol-Gel Sci Technol 14:27–38
34. Grassie N, Macfarlane IG, Francey KF (1979) The thermal degradation of polysiloxanes—II. Poly(methylphenylsiloxane). Eur Polym J 15:415–422
35. Vennemann N, Bokamp K, Broker D (2006) Crosslink density of peroxide cured TPV. Macromol Symp 245–246:641–650
36. Dong S, Gu K (2000) Influence of rubber composition on change of crosslink density of rubber vulcanizates with EV cure system by thermal aging. J Appl Polym Sci 75:1378–1384
37. Enns JB, Gillham JK (1983) Effect of the extent of cure on the modulus, glass transition, water absorptio, and density of an amine-cured epoxy. J Appl Polym Sci 28:2831–2846
38. Zhang CQ, Xia Y, Chen RQ, Huh S, Johnston PA, Kessler MR (2013) Soy-castor oil based polyols prepared using a solvent-free and catalyst-free method and polyurethanes therefrom. Green Chem 15:1477–1484
39. Nielsen LE (1969) Cross-linking–effect on physical properties of polymers. J Macromol Sci Part C 3:69–103
40. Abbasian A, Ghaffarian SR, Mohammadi N, Fallahi D (2004) The contact angle of thin-uncured epoxy films: thickness effect. Colloid Surface A Physicochem Eng Aspects 236:133–140

41. Martin HJ, Schulz KH, Bumgardner JD, Walters KB (2007) XPS study on the use of 3-aminopropyltriethoxysilane to bond chitosan to a titanium surface. Langmuir 23:6645–6651
42. Zhang H, Zhang J, Song S, Wu GF, Pu JW (2011) Modified nanocrystalline cellulose from two kinds of modifiers used for improving formaldehyde emission and bonding strength of urea-formaldehyde resinadhesive. BioResources 6:4430–4438
43. Sardon H, Irusta L, González A, Fernández-Berridi MJ (2013) Waterborne hybrid polyurethane coatings functionalized with (3-aminopropyl)triethoxysilane: adhesion properties. Prog Org Coat 76:1230–1235
44. Aran K, Sasso LA, Kamdar N, Zahn JD (2010) Irreversible, direct bonding of nanoporous polymer membranes to PDMS or glass microdevices. Lab Chip 10:548–552